CONTINUUM-BASED FEM MODELING OF CERAMIC POWDER COMPACTION [USING A CAP-PLASTICITY CONSTITUTIVE MODEL]

SAND2000-0266J

J. Guadalupe Argüello, A. F. Fossum, D. H. Zeuch and K. G. Ewsuk

Sandia National Laboratories

Albuquerque, New Mexico, USA

ABSTRACT

Software has been developed and extended to allow finite element (FE) modeling of ceramic powder compaction using a cap-plasticity constitutive model. The underlying, general-purpose FE software can be used to model even the most complex three-dimensional (3D) geometries envisioned. Additionally, specialized software has been developed within this framework to address a general subclass of axisymmetric compacts that are common in industry. The expertise required to build the input deck, run the FE code, and post-process the results for this subclass of compacts is embedded within the specialized software. The user simply responds to a series of prompts, evaluates the quality of the FE mesh that is generated, and analyzes the graphical results that are produced. The specialized software allows users with little or no FE expertise to benefit from the tremendous power and insight that FE analysis can bring to the design cycle. The more general underlying software provides complete flexibility to model more complicated geometries and processes of interest to ceramic component manufacturers but requires significantly more user interaction and expertise.

INTRODUCTION

Conventional ceramic component manufacturing often involves processing and fabrication with raw materials in powder form. Granulated powder is formed into a "green" body of the desired size and shape by consolidation, often by simply pressing nominally dry powder. Ceramic powders are commonly pressed in steel dies or rubber bags with the aim of producing a near-net-shape green body for subsequent sintering. Density gradients in these compacts, introduced during the pressing operation, are often severe enough to cause distortions in the shape of the part during sintering due to nonuniform shrinkage. In such cases, extensive green machining or diamond grinding may be required to produce a part with the desired final shape and size. In severe cases, density gradients and nonuniform shrinkage may even create cracks in the parts during sintering. Likewise, severe density gradients can result in green bodies that break during ejection from the die or that are too

DISCLAIMER

fragile to be handled during subsequent processing.

While empirical relationships (i.e., rules of thumb) exist to describe powder compaction, they do not provide the understanding necessary to control die design or compaction parameters to eliminate density gradients; consequently, the designer is forced to use expensive and time-consuming trial and error procedures to develop new components. The problem with this traditional approach is that compaction density gradients of unknown and uncontrolled magnitude are inevitably introduced in the process, contributing to warping and uncontrolled sintering, and ultimately to unpredictable component performance and reliability. For this reason, interest has grown in developing and applying computational tools to address the problem [1,2].

The technical approach that we have taken in this work has been to apply fundamental scientific understanding to develop an overall predictive model for powder compaction. A scientifically-based model should help us to design cost-effective processes to manufacture improved performance and reliability ceramics by providing the insight needed to control die design and/or compaction to minimize density gradients. The objective of this work, therefore, has been to develop an overall predictive model for powder compaction that will aid in producing components of accurate shape and size, as-sintered, without the need to perform extensive machining. We call this a "model-based design and processing" approach.

Development of our macroscopic, continuum-based, FE technology has involved four distinct steps:

- We identified and further developed a mathematical material description (i.e., constitutive model) capable of predicting ceramic powder consolidation response in the form of a multisurface plasticity model that is typically referred to as a cap-plasticity model [3];
- We identified, extended, and implemented a testing methodology to characterize ceramic powders in a manner consistent with the mathematical description to estimate parameters for the constitutive model;
- We implemented the constitutive model within a more general-purpose, established, and accepted numerical simulation technique (i.e., the finite element method, FEM) as embodied within the nonlinear, inelastic, large-deformation FE program, JAS3D [4]; and
- We validated the predictive capability afforded by the overall model to ceramic powder compaction.

The resulting tool is a powerful, predictive tool for ceramic powder compaction.

Beyond this, we also developed specialized software that wraps around various tools from Sandia's FE

toolkit, including the more general-purpose software. The specialized software targets a general subclass of axisymmetric compacts, typical of many commonly pressed parts. Its purpose is to provide a user-friendly, simple interface to the various tools in the FE toolkit that are typically needed to perform an analysis and to visualize/interpret the results from the FE analysis within the context of ceramic component manufacturing.

This paper will describe and discuss the details of each of the steps identified above to develop the underlying general FE technology and will delve into the specialized software that has been developed for nonexperts in the field of FE analysis.

CAP-PLASTICITY CONSTITUTIVE MODEL

Geotechnical engineers have had a rich and extensive history of providing tools to help evaluate soils behavior in the context of soil-structure interaction, a process that is analogous to the interaction of a ceramic powder with a metal die and/or rubber bag. For this reason, we began the search for a mathematical model of material behavior that might be applicable to ceramic powder compaction in the geotechnical literature. Among the many mathematical descriptions available, we sought one that could capture both the hydrostatic and deviatoric response of the powder; namely, one that could capture the compaction due to mean stresses (pressure) as well as the plastic flow and enhancement of compaction due to deviatoric stresses (shear). The justification for this is based on the analysis of a typical powder compaction curve obtained by uniaxial pressing relative to the measured density gradients in a die-pressed compact (Figure 1). The compaction curve in Figure 1a represents the average relative density obtained for a 94 wt% alumina body as a function of the applied compaction pressure. The fringe plot of relative density in Figure 1b was obtained by removing a central slice from a pressed alumina compact and determining spatial density using ultrasound velocity measurements. In this particular case, a 94 wt% alumina compact, 22.2 mm in diameter by 35.1 mm tall, was formed using a pressure of 68.9 MPa applied from the top. The highest relative density of 0.56 is measured in the upper right corner, as seen in the fringe plot. To reach such a compacted state implies that either the local "pressure" in that region was *significantly* higher than the applied 68.9 MPa or that the consolidation behavior of the powder is also influenced by the high deviatoric stresses occurring in that area due to friction between the powder and the die-wall. Because it is unlikely that higher pressure alone could account for the higher degree of compaction, a mathematical description of material behavior that allowed for the enhance-

ment of compaction was deemed necessary.

A model that captures the mechanical behavior of granular materials during consolidation, allowing for this enhancement of compaction, is the "cap-plasticity" model of Sandler and Rubin [3], shown schematically in Figure 2. The ordinate in this figure is the first invariant of stress (three times the mean stress or hydrostatic "pressure") and the abscissa is the second invariant of the deviatoric stress (a measure of the shearing stresses). Features of this model include two yield surfaces, one a stationary shear failure envelope, F_s, and the other a non-stationary strain-hardening cap, F_c, that bound the elastic regime. This allows for an initially "small" cap that grows and hardens during loading (compaction), an elastic rebound upon unloading (spring-back), and the possibility for secondary yielding (delamination) if unloading results in an intersection with the failure envelope. In Figure 2, material subjected to a stress state "Q" located on the cap would undergo the same effective compaction that material subjected to a stress state "X" on the cap; however the compaction of material at "Q" would be enhanced by the deviatoric component beyond what could be achieved by the hydrostatic component alone. Effectively, it "appears" that the material at "Q" is subjected to the higher purely hydrostatic stress state at "X."

The cap-plasticity model implemented and used in this work is a generalization of the Sandler-Rubin constitutive model. It was generalized so that it incorporates Lode-angle dependence of yield in the deviatoric plane and nonassociativity in the meridional plane on the shear failure surface. Details of this generalized model can be found in Argüello *et al.* [5]. The material model also includes a modified functional form of the pressure versus volumetric strain response to better-capture ceramic powder behavior.

The material parameters that define the surfaces and other pertinent characteristics of the model come from a combination of laboratory hydrostatic compression tests and from confined triaxial compression tests. Fossum *et al.* [6] have outlined the techniques by which hydrostatic and triaxial compression experiments are used to obtain parameters for models of the foregoing type.

CHARACTERIZATION OF CERAMIC POWDER MATERIAL RESPONSE

Hydrostatic compression experiments are performed to determine the evolution of the cap along the I_1 ($\sqrt{J_2} = 0$) axis, and to measure the bulk modulus at the pressure(s) of interest. The onset of permanent volume strain marks the initial location of the cap on the I_1 axis, and subsequent increases in pressure result in

permanent hardening. The initial bulk modulus, and those of the hardened states, are measured by monitoring strains during small depressurization/repressurization cycles at the corresponding pressures [7].

Triaxial compression experiments are used for several purposes. First, they are used to locate the position of the shear failure surface in $\sqrt{J_2}$ - I_1 space. The shear failure surface is usually (but not always) taken to be the loci of points in $\sqrt{J_2}$ - I_1 space outside of which the specimen will no longer support increasing deviatoric loads. Second, during deviatoric loading, small unload/reload cycles can be performed to measure Young's modulus and Poisson's ratio for the corresponding stress state [7]. Finally, by overhardening the specimens with a hydrostatic pressure sufficiently great to cause permanent strain, and then dropping to a lower pressure before deviatoric loading, the off-axis shape and evolution of the cap can be probed: Deformation within the cap-failure envelope wedge is elastic; when the "new" cap is reached, permanent shear and volumetric strain begin to accumulate.

Knowing the bulk and Young's moduli, and Poisson's ratio, the shear modulus can be calculated. Thus, all required parameters for the model can be obtained from these two types of experiments.

Our experiments, described in more detail in Zeuch *et al.* [8], were performed using a standard, liquid-medium, triaxial cell [7]. The cell consisted of a cylindrical, 200 MPa pressure vessel with one end of the closure penetrated by a moveable piston. The piston permitted application of a deviatoric load to a test specimen concurrent with a separately controlled hydrostatic pressure. For triaxial testing, this cell was mounted in a servo-controlled, 979 kN-capacity MTS frame that permitted transfer of load from the frame to the specimen. The cell was equipped with electrical feed-throughs that permitted direct strain measurements using various types of transducers, in this instance, linear variable displacement transducers (LVDTs).

Loose ceramic powders have very high porosities, so strains are large and inhomogeneous even under hydrostatic compression. Direct triaxial compression experiments on such specimens would not be useful because the initial state of the specimen (other than its density) would be poorly defined. For this reason, experiments on ceramic powders were conducted in two separate steps, which we call the hydrostatic and triaxial stages. In the first stage, the loose powders were compacted under a succession of hydrostatic pressures to establish pressure-density curves for each of the powders and to create a suite of pre-compacted specimens of known density and dimensions for the triaxial series. The specimen assembly consisted of a cylindrical,

44.5 mm inner diameter by 133.4 mm long Viton jacket, sealed with two aluminum endcaps fitted with O-rings. One endcap was vented to the atmosphere via a tube that penetrated the lower end closure to permit gas to escape from the specimen and test in the "drained" condition [7].

To prepare a specimen, a known weight of powder was poured into the rubber jacket-endcap assembly and vibrated for 60 seconds, followed by carefully assembling the vented endcap to the rubber jacket.

Volume measurements were then made on the assembly using Archimedes' method. The known volume of the jacket plus endcaps was subtracted out to determine the volume and density of the powder. The assembled specimen was then loaded into the pressure vessel, and successively pressurized to several different pressures. At the maximum pressure for each pressurization stage, a vacuum was applied to the specimen to keep the rubber jacket compressed tightly against the powder and the sample was removed from the vessel. Volume measurements were then made on the compacted specimen, and a density corresponding to that particular pressure was determined. The sample was then returned to the pressure vessel, and the specimen was pressurized to the next value in the series, until the final (*target*) pressure was reached. Typically, our target pressures were 6.9, 20.7, 34.5, 51.7, and 68.9 MPa. In this way, we determined the pressure-density curves for the powders up to 68.9 MPa and also obtained a suite of pre-compacted specimens of known density that were subsequently machined into cylinders of known length and diameter for triaxial testing.

For triaxial testing, the hydrostatically pressed cylindrical specimens were jacketed in polyolefin tubing and sealed with endcaps, with the lower endcap again vented. The endcaps were equipped with holders for a pair of diametrically opposed LVDTs to measure axial strain. A single spring-loaded LVDT held in a clip-on fixture measured diametral strain.

This assembly was returned to the triaxial test cell, and pressurized back to the highest pressure that the specimen experienced during the hydrostatic stage. Once the target pressure was reached, a depressurization/pressurization cycle was performed to measure the bulk modulus. The absolute magnitude of the pressure cycle depended on the target pressure, with larger loops possible at higher pressures. To preserve the original state of the specimen, it was never completely depressurized during the depressurization-pressurization loop.

For triaxial testing, the moveable piston was brought into contact with the specimen endcap and then moved at a constant displacement rate corresponding to a nominal axial strain rate of 1×10^{-4} s^{-1}. During the

course of the axial deformation, the specimen was partially unloaded and reloaded periodically to measure Young's modulus and Poisson's ratio. Again, the magnitude of the cycle depended on the confining pressure and strength of the specimen. Pronounced "barreling" of the specimens was observed under all test conditions, and axial stresses were continuously corrected for the change in cross-sectional area.

FINITE ELEMENT DISCRETIZATION

The cap-plasticity constitutive model described can be incorporated into simple mathematical algorithms to model specific simple geometries and compacts of academic interest; however, for application to problems that are of interest to ceramic component manufacturers, a much more general tool was needed. Realistically, a useful tool has to be able to capture the varied and complex geometries of real pressed parts; the general loading and unloading conditions that are imposed when those parts are manufactured; and the general initial and boundary conditions that must be imposed to yield a desired part. A general-purpose, established, and accepted numerical simulation technique that provides this functionality is the finite element method. In particular, the advanced quasistatic FE technology developed by Sandia National Laboratories that is based on iterative solvers has been a key element in our program. This technology has been specifically and extensively developed under defense programs to handle large problems involving large deformations, exactly the type of problem typically encountered when simulating the pressing of ceramic components. The use of iterative solvers and the extensive experience with non-linear material response that exists at Sandia provided a base technology that offered an efficient solution to this type of problem.

For the displacement-based FEM used in this work, the field equations governing deformation of a body can be discretized and written as [5]:

$$\left\{ \sum_{N} \int_{ve} \mathbf{B}\sigma dV \right\} = \{\mathbf{F}\}, \text{ or } [\mathbf{K}(\mathbf{u})]\{\mathbf{u}\} = \{\mathbf{F}\}, \tag{1}$$

where the term on the left-hand side of each form of the equation is the internal force vector, and $\{\mathbf{F}\}$ is the external force vector. In the first form, $\mathbf{B}$ is the strain-displacement transformation matrix, N is the number of elements in the FEM discretization, σ is an ordered vector of stress components in each element at a Gauss point, and *ve* is the volume of each element. In the second form of Equation (1), on the right, $[\mathbf{K}(\mathbf{u})]$ represents the global stiffness matrix in the traditional FEM [9] and $\{\mathbf{u}\}$ represents the global vector of unknown

nodal displacements. Both forms of the equation are included to highlight the differences in approach between the traditional FEM approach and the explicit approach used in this work within the quasistatic non-linear FE program, JAS3D [4]. The stress-strain relationship (constitutive model) is incorporated via the integrand product in the left-hand side of the first form of Equation (1) and is similarly incorporated within the left-hand side of the second form as well. The cap-plasticity constitutive model described above was implemented within JAS3D in the form of a material subroutine and constitutes one of many material models available in the code for simulating various advanced industrial processes.

The explicit technology that forms the basis of the present work approaches the solution of Equation (1) in a manner different from that used in the traditional FEM [9]. First, a global stiffness matrix is never formed. Instead, at the element level, the divergence of the stress is found, and the contributions to each node in the overall structure are summed (i.e., the vector described by the left side of the first form of the equation). A residual force vector comprised of the internal minus the external forces,

$$\{R\} = \left\{ \sum_{N} \int_{ve} B\sigma dV \right\} - \{F\}, \tag{2}$$

is computed, and the solution procedure is then one of reducing the residual to zero using an iterative technique. Because the quantities being manipulated are vectors, there is no need to store a global stiffness matrix and factor it. Consequently the storage requirements are small when compared to the traditional FEM approach and larger problems can be solved more efficiently. The two iterative techniques that are currently used in JAS3D are a pre-conditioned Conjugate Gradient (CG) technique [10] and an adaptive Dynamic Relaxation (DR) technique [11].

MODEL VALIDATION FOR SIMULATING POWDER COMPACTION

Once the cap-plasticity model was implemented within JAS3D, confidence needed to be established in the accuracy of the overall model for predicting powder compaction response. Although JAS3D continuously undergoes many specific processes to improve software quality (e.g., change control, configuration control, regression testing, etc.), its predictive capability using the newly implemented constitutive model needed to be ascertained.

The first check performed was to simulate one of the laboratory tests performed on the 94 wt% alumina.

The triaxial test at 68.9 MPa confining pressure was chosen and the entire loading history of the material was simulated, i.e., hydrostatic loading to target confining pressure followed by an increasing axial load thereafter. The simulation was performed using the material parameters obtained from all the hydrostatic and triaxial tests completed on this specific powder. Figure 3a shows the results of the JAS3D simulation overlaid on the data from the laboratory experiment. Axial stress is plotted as a function of the axial and radial components of strain. With the obvious exception that the JAS3D simulation did not include any of the unload/reload cycles seen in the data, the figure shows that there is good agreement between the simulation and the experiment. During the phase of hydrostatic loading to the target confining pressure of 68.9 MPa, all components of strain are equivalent. However as the axial stress increases beyond the confining pressure, during the actual triaxial phase of the test, the axial strain continues to increase while the radial strain begins to decrease. In both the simulation and experiment, the maximum value of axial stress reached is about 172.4 MPa.

With confidence that the cap-plasticity model had been implemented correctly within JAS3D, a more complex simulation was performed. The uniaxial compaction of the cylindrical specimen shown in Figure 1b was undertaken assuming a compaction ratio of about 1.9 (i.e., the powder fill height was 67 mm). This is more complicated because we have to account for the interaction of the powder with the die-wall. The contact interaction in JAS3D was modeled simply with Coulomb friction and the coefficient of friction between the die-wall and the powder was assumed to be 0.2, which is within the range of values measured for the interaction of ceramic powders with various die-wall materials. Because of symmetry and an assumption of uniformity in die-filling, only a wedge of the cylinder needed to be modeled with JAS3D. The fringe plot of computed relative density from this simulation is shown in Figure 3b. The computed relative density at the outer top of the compact is 0.56- 0.57, while that at the outer bottom is 0.50-0.51. These predictions compare quite well with the respective measured values of 0.56 and 0.50 in Figure 1b. The spatial distribution of relative density, however, is somewhat different, particularly in the radial direction near the top and bottom of the cylinder. This may be attributable to several things, among them the manner in which the upper and lower boundaries were specified in the simulation. In the simulation, material was free to move radially but not axially relative to the vertically moving boundary at the top and the stationary boundary at the bottom. In the real pressing scenario, there are platens at the top and bottom that also interact with the powder and will induce

shearing stresses. Furthermore, a uniform die-fill was assumed in the simulation that is undoubtedly not the case in the real part: this can be inferred by the presence of asymmetry in the density distribution relative to the axis of the cylinder in Figure 1b. Finally, the coefficient of friction between the die-wall and the powder may be different from the assumed value, or the frictional interaction may not be simple Coulomb friction.

Additional simulations have been performed on more complex geometry compacts to gain further confidence in the predictive capability of the overall model, and we have had a similar degree of success in predicting density distributions. Ultimately, however, the real test of the model's predictive capability will be at the hands of ceramic component manufacturers who must gain confidence in this tool by comparing code predictions with measured data from a wide range of production parts.

SPECIALIZED SOFTWARE

The resulting tool above can be used to predict forming stresses, density gradients, and material flow to investigate the effects of compact geometry; compaction ratio; pressing conditions (single, dual, hydrostatic pressing); die-wall friction coefficient; and die design (tapers, corner radii, etc.). As such, it constitutes part of the general underlying software, that we will refer to as the Sandia FE "toolkit" that is available to model even the most complicated 3D ceramic compacts envisioned. Effective use the software at this level, however, requires significant FE modeling expertise, insight into the underlying mechanics of the compaction process, and experience in using the cap-plasticity constitutive model and the JAS3D code. Furthermore, constructing the FE mesh that is part of the required input to JAS3D as well as visualizing results from the database output from JAS3D depends on several additional pre- and post-processing tools from the toolkit.

These significant requirements and potential impediments for using the underlying software, by the typical engineer on the production floor, called for a more user-friendly tool than the general-purpose capability described. To achieve this goal, it became essential to limit the scope of the class of problems to be handled by the software without being overly restrictive. The flexibility to model simple and complex geometry dies was achieved by developing higher-level specialized software to wrap around the general toolkit to address geometry variability within the axisymmetric subclass of compacts that are quite common in the industry.

This was accomplished by allowing multiple concentric cylinders to be stacked axially, as depicted schematically for three cylinders in Figure 4. The cylinders are interconnected using smaller transition radii that

can be varied systematically. The individual cylinders, which can be solid or hollow, are allowed to have variable inner and outer diameters and heights. By linking the different size and shape cylinders axially, it is possible to model geometric features like counter-bores and bushing stems that are common in complex-geometry ceramic components fabricated by powder pressing. In addition to the geometric variables mentioned, the software also provides some capability to realistically vary the properties of the die and powder compact materials, as well as the loading applied to the compacts.

At the heart of the software we call "UNIPACK" is a top-level driver that queries the user, builds and parses input parameter files, and wraps around Sandia's existing FE analysis toolkit to automatically perform a ceramic powder compaction analysis. In addition, there are key, pre-built files that contain the logic to generate the mesh for the compact in question from the input geometric quantities.

The overall flow of the specialized UNIPACK software package is depicted in Figure 5. There are three distinct phases that are automatically handled by the software:

- Geometry Definition Phase – Queries user for geometry information, builds user parameter files, and parses these files to the FE pre-processing tools to build the FE mesh for use in the analysis.
- Run Definition Phase – Queries user for parameters that define pressing conditions and type of material (specific powder) being pressed; builds a file of user parameters, and parses this file to a pre-processing tool to build an input deck for JAS3D.
- Solution & Post-processing Phase – Submits the FE analysis run; after the analysis finishes, it calls the FE post-processing tool to query the FE results database and generates a postscript file of select results; it then launches a postscript viewer to display this file to the user.

Thus, the expertise required to build the input deck, run the FE analysis code, and post-process the results resides in the specialized package. The user simply responds to a series of prompts, evaluates the quality of the FE mesh that is generated automatically, and analyzes the graphical results generated from the simulation.

Figure 6 shows a two-piece part simulated with the specialized software. Figure 6a is a schematic of the problem, showing that very few parameters are needed by the software to perform the simulation (ten radii, two heights, etc.). Figure 6b is an actual postscript image of results from the simulation that is presented to the user at the end of the simulation. In this case, it is a fringe plot of relative density; i.e., relative to the start-

ing density. This relatively small simulation takes about 30 minutes of CPU time to run under the Linux OS on a 450 MHz Pentium III PC.

This specialized software tool allows users with little or no FE expertise to benefit from the tremendous power and insight that FE analysis can bring to the design cycle. Furthermore, as the user develops expertise in modeling the powder compaction process with the specialized software package, the more general underlying software is available to him to allow modeling of more complicated geometries and processes.

SUMMARY AND CONCLUSIONS

A cap-plasticity constitutive model, originally developed to predict the geomechanical response of soils, has been adapted to simulate the compaction of ceramic powders. The parameters for the constitutive model are obtained from an extensive suite of hydrostatic and triaxial compression "soils-like" laboratory tests on specific ceramic powders. The constitutive model has been implemented in a finite element program for simulating the quasistatic, nonlinear, large deformation, inelastic response of solids. The overall tool has been used to predict and investigate the response of different powder compacts to various die-design details and parameters and pressing conditions. Thus the overall model has been at least qualitatively validated for ceramic powder compaction, and additional efforts are underway to further exercise and obtain increased confidence in its predictive capability.

Recent efforts have focused on developing a "user-friendly" powder compaction "package" in which the "expertise" required to perform the highly nonlinear analyses on a subclass of axisymmetric "complex" parts is embedded within the system and invisible to the user. A "test-of-concept" version of the software package for die-pressed compacts, running under Linux on a PC, has been demonstrated and was released to our industrial partners. In turn, they will exercise the specialized software; compare its predictive capability to production parts; and suggest improvements for the package. Generalization of the specialized software to include biaxial-pressing and bag-pressing is also currently underway.

ACKNOWLEDGMENTS

The authors thank Mark Grazier of Sandia National Laboratories for completing the hydrostatic and triaxial compression tests on the alumina powder, Donald Ellerby and C. M. Stone of Sandia National Laboratories for providing a critical review of this manuscript, and the members of AACCMCI, Inc. for their assistance

with testing and validating the compaction model. This work was funded by the US Department of Energy under contract No. DE-AC04-94AL85000. Sandia is a multiprogram Laboratory operated by Sandia Corporation, a Lockheed Martin Company.

REFERENCES

1. Aydin, I., B. J. Briscoe, and K. Y. Sanliturk, "The Internal Form of Compacted Ceramic Components: A Comparison of a Finite Element Modelling with Experiment." *Powder Technology*, 89:239-254, 1996.
2. Coube, O., *Modelling and Numerical Simulation of Powder Die Compaction with Consideration of Cracking*, Ph.D. Thesis, University Pierre et Marie Curie, Paris VI, 1998.
3. Sandler, I. and D. Rubin, "An Algorithm and a Modular Routine for the Cap Model," *Int. J. Numer. Anal. Methods Geomech.*, 3:173-186, 1979.
4. Blanford, M. L., *JAS3D - A Multi-Strategy Iterative Code for Solid Mechanics Analysis, User's Instructions, Release 1.6*, Internal Sandia Report, Sandia National Laboratories, Albq., NM, 1999.
5. Argüello, J. Guadalupe, C. M. Stone, and A. F. Fossum, "Progress on the Development of a Three-Dimensional Capability for Simulating Large-Scale Complex Geologic Processes," *Int. J. Rock Mech. Min. Sci.*, Vol. 35 4/5:469-470, Paper No. 083, 1998.
6. Fossum, A. F., P. E. Senseny, T. W. Pfeifle, and K. D. Mellegard, "Experimental Determination of Probability Distributions for Parameters of a Salem Limestone Cap Plasticity Model," *Mech. of Mat.*, 21:119-137, 1995.
7. Jaeger, J. C. and N. G. W. Cook, *Fundamentals of Rock Mechanics*, 3rd ed., Chapman and Hall, London, England, 1979.
8. Zeuch, D. H., J. M. Grazier, J. G. Argüello, and K. G. Ewsuk, "Measurement of the Mechanical Properties and Shear Failure Surfaces of Two Alumina Powders in Triaxial Compression," in preparation, 2000.
9. Crisfield, M. A., *Non-linear Finite Element Analysis of Solids and Structures (Vol. 1)*, John Wiley & Sons, Chichester, UK, 1991.
10. Biffle, J.H., *JAC3D - A Three-Dimensional Finite Element Computer Program for the Nonlinear Quasistatic Response of Solids with the Conjugate Gradient Method*, SAND87-1305. Sandia National Laboratories, Albq., NM, 1993.

11. Stone, C. M., *SANTOS - A Two-Dimensional Finite Element Program for the Quasistatic, Large Deformation, Inelastic Response of Solids*, SAND90-0543, Sandia National Laboratories, Albq., NM, 1997.

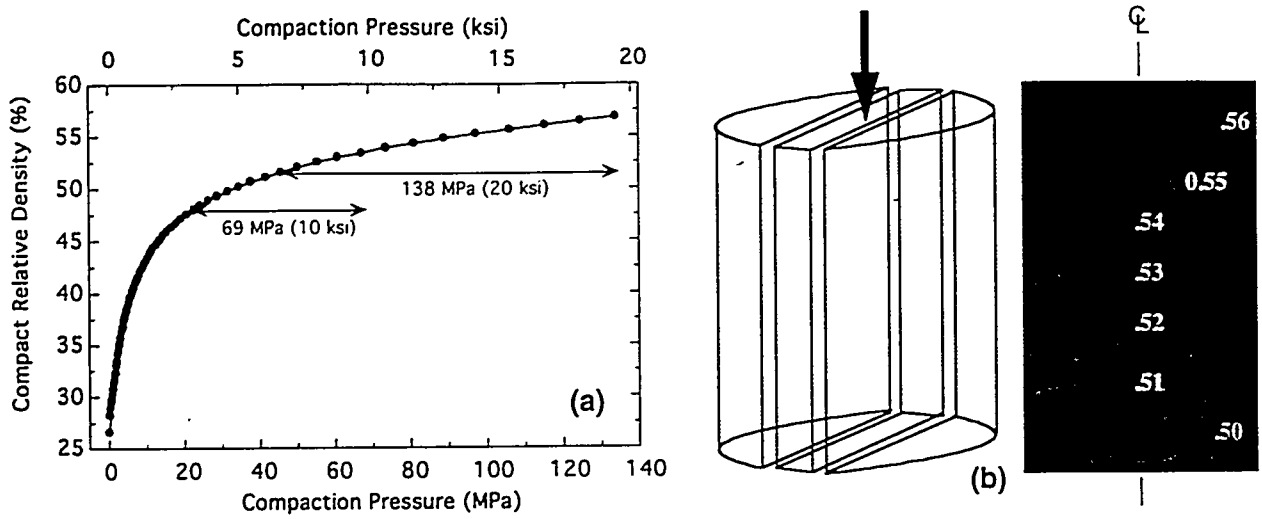

Figure 1: Measured (a) Powder Compaction Curve and (b) Density Gradients for a 94 wt% Alumina Compact Top–Pressed to 68.9 MPa.

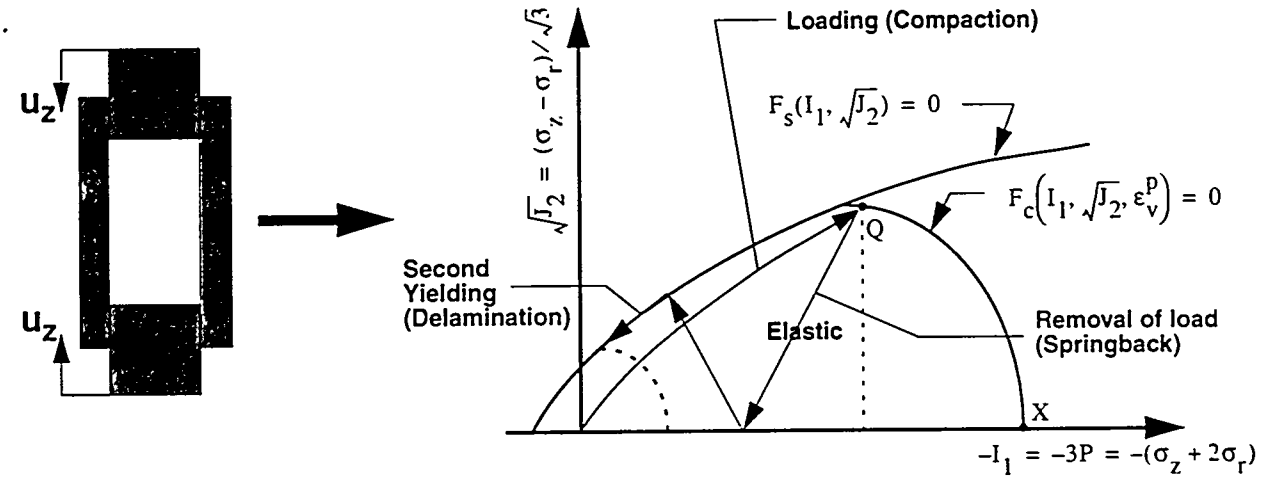

Figure 2: Schematic of Material Response Captured by Cap-Plasticity Model.

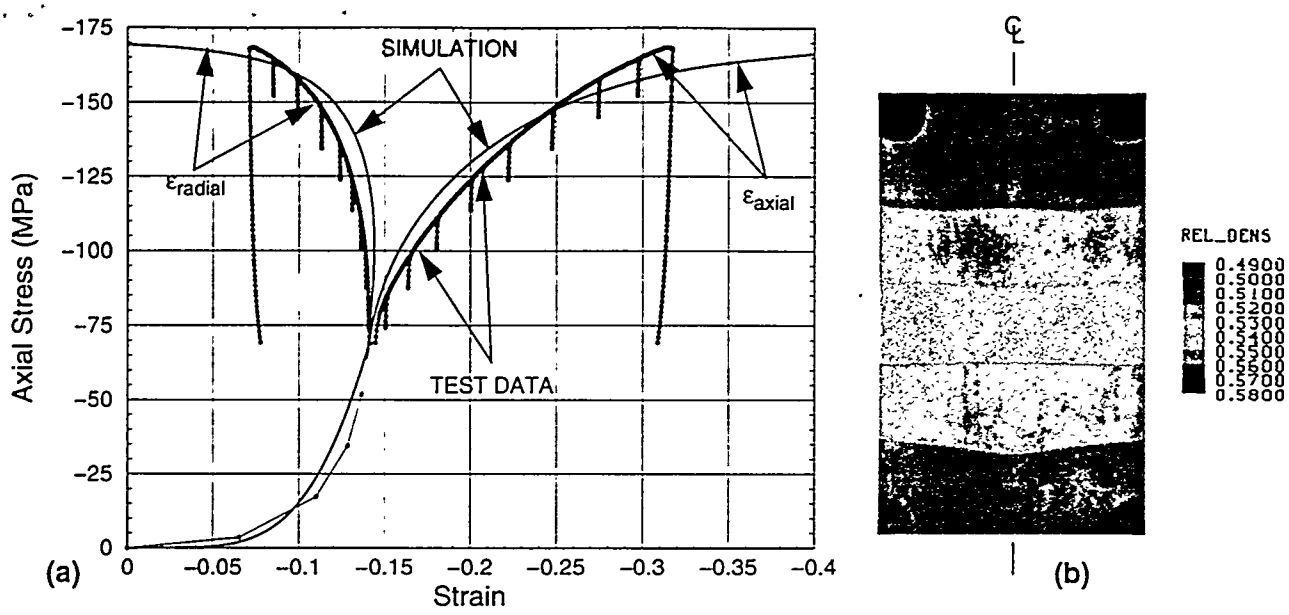

Figure 3: (a) Comparison of Data from Confined (68.9 MPa) Triaxial Compression Test with a JAS3D Simulation (b) Fringe Plot of Computed Relative Density for the Uniaxially Compacted Cylinder in Figure 1b.

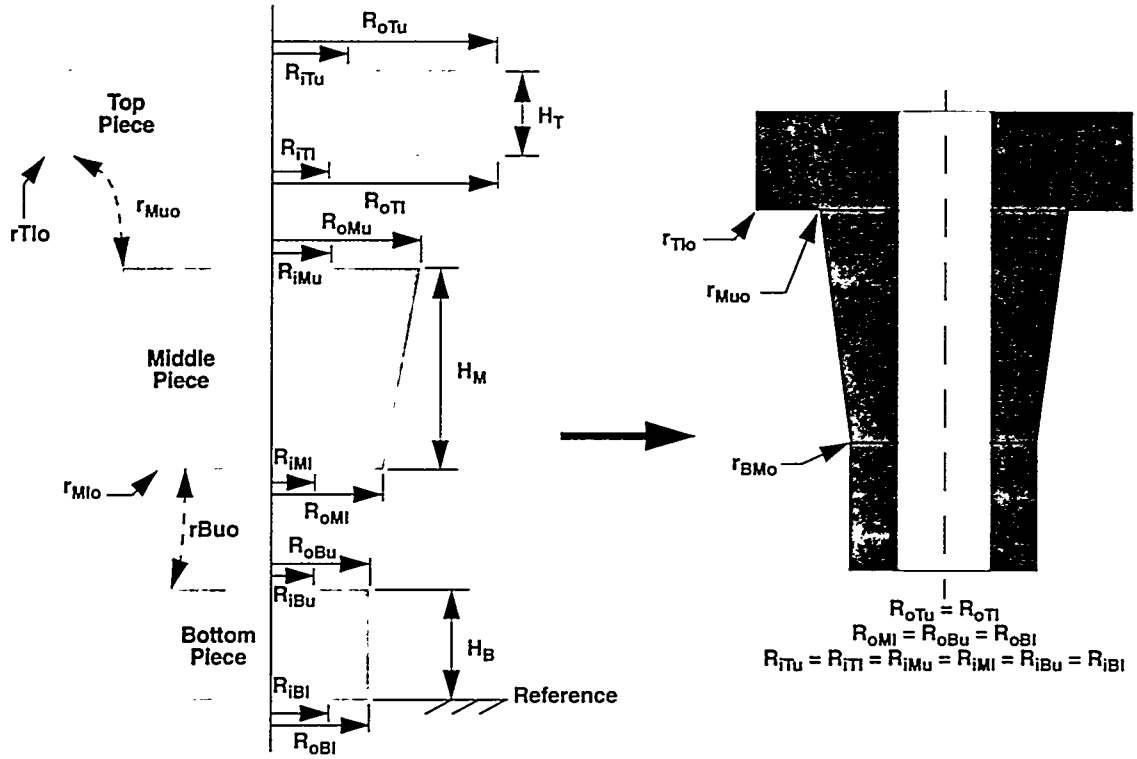

Figure 4: Schematic of a Complex Part Built Up from Three Stacked Axisymmetric Pieces.

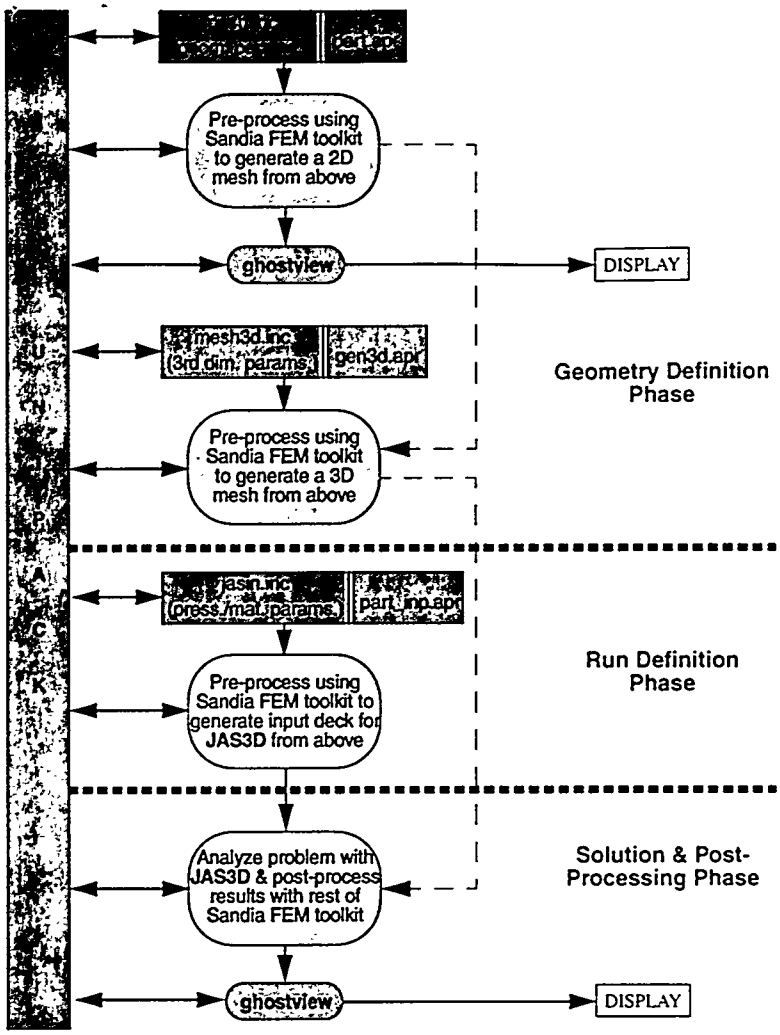

Figure 5: Flow Diagram Depicting How Unipack Drives and Wraps Around Existing Tools from the Sandia Finite Element Toolkit.

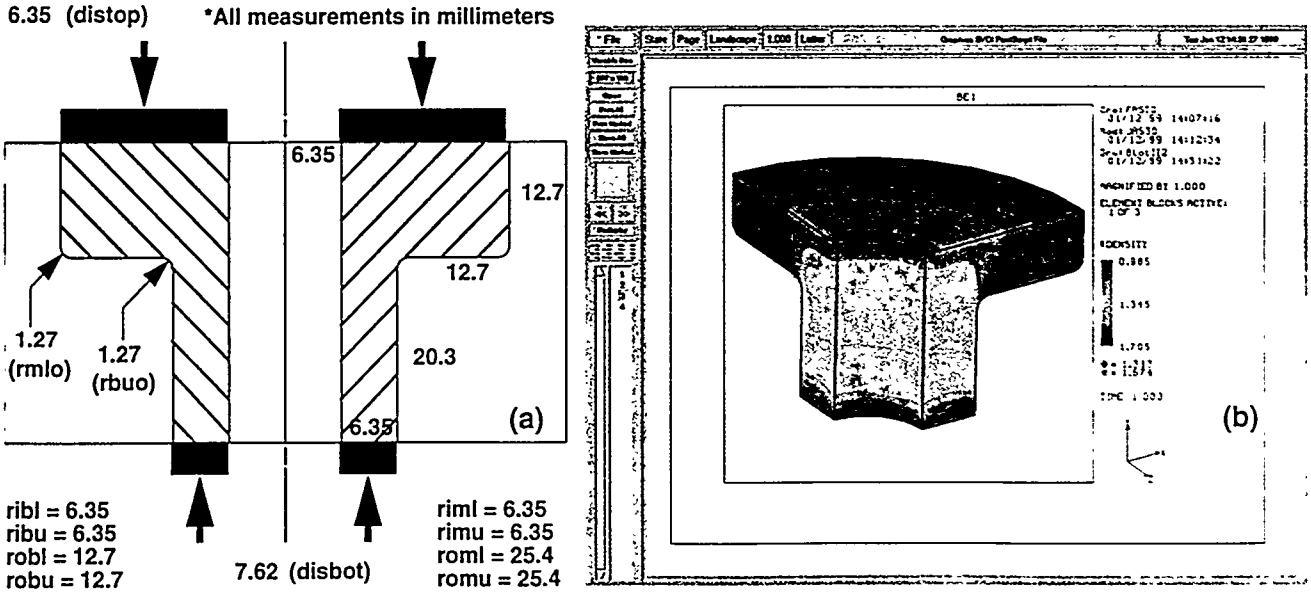

Figure 6: Sample Two-Piece Compact Simulated with Specialized Software (a) Parameters Needed by Package (b) Postscript Image of Density Fringe Plot from the Simulation.